

THE APTLY NAMED PHOENIX DWARF GALAXY

LISA M. YOUNG,

Physics Department, New Mexico Tech, 801 Leroy Place Socorro, NM 87801

EVAN D. SKILLMAN, DANIEL R. WEISZ,

Astronomy Department, University of Minnesota, 116 Church St. SE, Minneapolis, MN 55455

AND

ANDREW E. DOLPHIN

Department of Astronomy/Steward Observatory, 933 N. Cherry Ave., University of Arizona, Tucson, AZ 85721-0065; Raytheon Company

ApJ, accepted 27 December 2006

ABSTRACT

The Local Group galaxy Phoenix has the properties of a dwarf spheroidal galaxy, but an adjacent HI cloud has been recently found to be at the same radial velocity as the stars. The proximity suggests that this cloud is associated with the most recent (≤ 100 Myr) star formation in Phoenix. We have obtained relatively high sensitivity and high resolution HI imaging with the VLA with the goal of distinguishing between different processes for displacing the gas from the galaxy. Due to the outer curvature of the HI cloud, it appears that expulsion from the galaxy by winds from supernovae is more likely than ram-pressure stripping. The isolation of the galaxy makes tidal stripping highly unlikely. Using a star formation history constructed from HST imaging, we construct a simple kinematic model which implies that the HI cloud is still gravitationally bound to the galaxy. Gas which is expelled from the centers of dwarf galaxies but which remains gravitationally bound may explain the episodic star formation observed in several dwarfs. In the specific case of Phoenix, there may be future star formation in this currently dSph-like galaxy.

Subject headings: galaxies: individual (Phoenix dwarf) — galaxies: dwarf — galaxies: ISM — galaxies: kinematics and dynamics — galaxies: evolution

1. INTRODUCTION

The Local Group dwarf galaxies are an intriguing puzzle. Most of them can be divided into two different families: the dwarf spheroidals (which show no HI gas, no current star formation, and no sign of rotational support) and the dwarf irregular galaxies (which are HI rich, and show obvious signs of recent star formation and a significant degree of rotational support). In the last decade it has become clear that the dwarf spheroidals show a large range in star formation histories— some of them are dominated by old (~ 10 Gyr) stellar populations, but many have large components of intermediate age (~ 5 Gyr) and even some young (≤ 1 Gyr) stars (Mateo 1998; Grebel 2001; Dolphin et al. 2006). Stellar abundance patterns also show that in many cases the process of recycling interstellar gas into new stars must have continued over multiple Gyr (e.g., Ikuta & Arimoto 2002; Venn et al. 2004; Fenner et al. 2006). Thus, 5 billion years ago, many of the galaxies which we call dwarf spheroidals must have been significantly more gas-rich than they are now and they may have looked very much like today’s dwarf irregulars. What mechanism or mechanisms are responsible for transforming the dwarf spheroidals into their current state?

The fate of the neutral gas in the smallest galaxies is relevant to cosmological problems of current interest,

such as the chemical enrichment history of the early universe. Additionally, it may offer insight into the “dwarf galaxy number crisis”— the prediction from standard cosmologies that hundreds of unidentified dark matter halos should inhabit the Local Group (Moore et al. 1998; Klypin et al. 1999). A long favored theory holds that bursts of star formation can remove the ISM from a dwarf galaxy because of the small gravitational potential depth (e.g., Larson 1974; Vader 1986; Dekel & Silk 1986). However, recent hydrodynamical simulations of bursts in dwarf spheroidal systems imply that removing all of the ISM may be difficult to accomplish in practice (Mac Low & Ferrara 1999; Marcolini et al. 2006). This theory may also require some delicate fine-tuning in order to explain a galaxy like the Carina dwarf, which shows evidence of three well isolated episodes of star formation (Saha et al. 1986; Mighell 1990; Smecker-Hane et al. 1994; Mighell 1997). If the star formation activity is energetic enough to clear gas from the galaxy, then either fresh gas was re-accreted between episodes or the clearing is only partial.

Ram pressure stripping presents a second viable theory, and it has the advantage of naturally explaining the morphology-density relationship observed for the Local Group dwarfs (e.g., Einasto et al. 1974; Lin & Faber 1983; Kormendy 1985; van den Bergh 1994a,b). Recently, Mayer et al. (2001a,b, 2006) have suggested that ram pressure plus “tidal stirring” (the combined effects on a satellite galaxy during passage through perigalacticon) can convert a dwarf irregular into a dwarf spheroidal

Electronic address: lyoung@physics.nmt.edu
Electronic address: skillman@astro.umn.edu, dweisz@astro.umn.edu
Electronic address: adolphin@raytheon.com

by inducing a burst of star formation while simultaneously heating the stellar disk and pulling off the ISM in a tidal stream. These processes are most important, though, on orbits with pericenters less than 50 kpc.

High resolution and high sensitivity HI observations provide a probe to examine which processes are responsible for removing the gas from the galaxy. For ram pressure stripping, one expects the gas to be displaced in the opposite direction to the galaxy’s motion. One might also expect that on the side of the cloud facing the optical galaxy there would be a stronger column density gradient giving a bow shock appearance similar to Ho II (Bureau & Carignan 2002) and the LMC (de Boer et al. 1998). For blow-away, naively, one expects gas ejected in more than one direction and possibly the presence of a bow shock pointed away from the galaxy. For tidal stirring, one expects an elongated tidal feature.

The Phoenix dwarf offers a unique opportunity in the study of the mechanisms that can transform a gas-rich dIrr into a gas-poor dSph. Its stellar population is primarily old, but some star formation activity has continued until about 100 Myr ago (Ortolani & Gratton 1988; Martínez-Delgado, Gallart, & Aparicio 1999). There is also an HI cloud which is associated with the galaxy (Young & Lo 1997; St-Germain et al. 1999; Gallart et al. 2001) but displaced from the stellar body, and this arrangement suggests that whatever processes are responsible for gas removal might be taking place right now in Phoenix. The other nearby dwarf galaxies have either lost their gas long ago, so that no signs of the removal process remain, or they still retain their gas, so that no signs of the removal process are visible yet.

The first map of the -23 km s^{-1} HI cloud now believed to be associated with the Phoenix dwarf was presented by Young & Lo (1997) at $133'' \times 102''$ resolution. Subsequent mosaic imaging by St-Germain et al. (1999) had comparable sensitivity and resolution ($180'' \times 180''$) but much better recovery of large scale ($\gtrsim 10'$) HI structures in the region. At the time, the radial velocity of the Phoenix dwarf was not known, but more recent velocities from stellar spectra (Gallart et al. 2001; Irwin & Tolstoy 2002; Held 2002) showed an excellent match with the HI radial velocity, securing the association. Comparisons of the properties of the -23 km s^{-1} cloud with the other nearby gas clouds provided evidence that the -23 km s^{-1} cloud is indeed physically associated with the Phoenix dwarf and that the others are almost certainly foreground emission. We now present very deep VLA integrations on the -23 km s^{-1} cloud which give a factor of three better sensitivity at improved resolution ($71'' \times 71''$). We use these high quality images to study the detailed structure of the cloud and to seek clues, as described above, to the physical mechanisms responsible for the evolution of the interstellar medium in the Phoenix dwarf.

The distance to the Phoenix dwarf has been very well constrained by observations of its tip of the red giant branch stars since the pioneering work of van de Rydt et al. (1991), who first derived a distance modulus of 23.1 ± 0.1 . Subsequent studies have all been consistent with this value as Martínez-Delgado, Gallart, & Aparicio (1999) derived 23.0 ± 0.1 , Held et al. (1999) derived 23.04 ± 0.07 (and a value of 23.21 ± 0.08 based on the luminosity of the horizontal branch stars), and Holtzman et al. (2000) de-

rived a value of 23.11 with an uncertainty of “several percent.” As described in §4, we have re-analyzed imaging from the HST archive, and find a distance modulus of 23.11 ± 0.05 (or, roughly 420 ± 10 kpc). We will use this distance throughout the paper.

2. OBSERVATIONS AND DATA REDUCTION

The first interferometric HI observations of the Phoenix dwarf consisted of 2.0 hours with the National Radio Astronomy Observatory’s Very Large Array¹ in the DnC configuration on 1996 May 18 and 4.0 hours in the CnB configuration on 1996 Jan 23. The results of those data are published in Young & Lo (1997).

Additional observations in 2003 and 2004 were, in total, four times longer than the 1996 data. The Phoenix dwarf was observed for a total of 12.0 hours in the DnC configuration on 2003 Jan 24, 25, and 27 and for another 12.0 hours in the CnB configuration on 2004 Jan 23, 24, and 25. All data were obtained with a total bandwidth of 1.56 MHz, giving 256 channels of 6.1 kHz (1.3 km s^{-1}) each. The velocity range covered is $+188.7 \text{ km s}^{-1}$ to -74.2 km s^{-1} (heliocentric, in the optical definition). Integration times were 60 seconds on source in the DnC configuration and 20 seconds on source in CnB. The nearby point source J0155-408 was observed every 40 minutes as a phase reference; the bandpass and flux calibration data were obtained from the source J0137+331.

All data calibration and image formation were done using standard calibration tasks in the AIPS package. Initial imaging revealed which channel ranges were free of HI line emission. Continuum emission was subtracted directly from the raw visibility data by making first order fits to the line-free channels. All datasets were then combined. For a low resolution map (described in greater detail below), the datasets were combined with no change to their nominal weights. For a higher resolution map the data weights in the 2004 CnB observations were multiplied up by a factor of two. This upweighting partly offsets the lower weights resulting from the shorter integration times in the CnB array so that after final gridding in the visibility plane, both DnC and CnB configurations contribute roughly equally to the final image.

The primary imaging difficulty for VLA imaging of the Phoenix dwarf is in achieving a nearly round synthesized beam for a source of such low declination. The beam is elongated in the north-south direction even for data from the DnC configuration, so, in effect, the north-south baselines from the CnB configuration are used in combination with the east-west baselines from the DnC configuration to create a synthesized beam which is nearly round. A low resolution cube was made using the “natural” weighting scheme (data weights do not depend on the local density of samples) applied with a Gaussian taper to downweight long baselines. The resulting beam had a fitted FWHM of $130'' \times 116''$. The dirty image was cleaned down to a residual level of approximately 1.0 times the rms noise fluctuations, and clean components were restored with a circular beam of FWHM $130''$. A higher resolution cube was made using Briggs’s robust weighting scheme (Briggs, Schwab, & Sramek 1999), as

¹ The National Radio Astronomy Observatory is a facility of the National Science Foundation operated under cooperative agreement by Associated Universities, Inc.

TABLE 1
IMAGE PARAMETERS

	high res	low res
uvtapers (k λ)	3, 50	1, 3
robustness	2	5
“original” beam FWHM (″)	71 \times 52	130 \times 116
“original” beam PA (°)	14	57
restoring beam FWHM (″)	71 \times 71	130 \times 130
Linear resolution (pc)	140	260
rms noise (mJy b $^{-1}$)	1.2	1.9
N(HI) sensitivity (cm $^{-2}$)	2.0 \times 10 18	9.6 \times 10 17

NOTE. — Column density sensitivities are 3σ in one channel.

implemented in the AIPS task IMAGR with a robustness parameter 2, plus an additional Gaussian taper to downweight baselines extended in the east-west direction. The synthesized beam for this image had a fitted FWHM of $71'' \times 52''$. It was cleaned in the same manner as the low resolution cube and restored with a round beam of FWHM $71''$. Offline Hanning smoothing produced channels of width 2.6 km s^{-1} for both cubes. Additional imaging details and final sensitivities are given in Table 1.

Integrated intensity (zerth moment) maps were made by the masking method: the deconvolved image cube was smoothed along both spatial and velocity axes, and the smoothed cube was clipped at about 1.0σ (the noise level before smoothing) in absolute value. The clipped version of the cube was used as a mask to define a three-dimensional volume in which the emission is integrated over velocity. Integrating the “moment zero” image again over the spatial directions then gives the total HI flux.

The low resolution HI cube contains a total of $2.95 \pm 0.05 \text{ Jy km s}^{-1}$ of HI emission in the vicinity of the Phoenix dwarf. The uncertainty in this value is indicative of the variability that results from slightly different sum regions. The higher resolution HI cube contains a total of $2.8 \pm 0.1 \text{ Jy km s}^{-1}$, which is entirely consistent with the flux in the low resolution cube. Both values are just a bit higher than the 2.6 Jy km s^{-1} measured by Young & Lo (1997) in their lower sensitivity data cubes. Accounting for uncertainty in the absolute flux calibration, we count a total flux of $2.95 \pm 0.10 \text{ Jy km s}^{-1}$ from the Phoenix dwarf. In comparison, St-Germain et al. (1999) quote 4.0 Jy km s^{-1} in this cloud, so the new VLA maps have recovered at least 75% of the HI flux. At 420 kpc, this flux corresponds to $1.2 \times 10^5 M_{\odot}$ of HI.

3. THE SPATIAL AND KINEMATIC STRUCTURE IN THE PHOENIX HI CLOUD

As in previous observations of the region, Galactic emission is detected in the velocity range $+16$ to -2 km s^{-1} . The southern clouds noted by Young & Lo (1997) and St-Germain et al. (1999) are also evident in the velocity range $+44$ to $+75 \text{ km s}^{-1}$. However, since these clouds are not believed to be associated with the Phoenix dwarf we do not discuss them further.

Our new images confirm the general impressions gained from earlier, lower resolution and lower sensitivity data but provide important new details on the internal struc-

ture of the gas cloud associated with Phoenix. For example, Figure 1 shows the integrated HI intensity of the -23 km s^{-1} cloud at $71''$ resolution. At column densities $\sim 10^{19} \text{ cm}^{-2}$ the angular extent of the cloud is roughly $8' \times 8'$, similar to that noted by St-Germain et al. (1999). However, the curved shape of the cloud is much more obvious here than in the low resolution images. The new data also reveal that the “center of curvature” of the cloud is *not* coincident with the optical center of the galaxy; rather, it is some $2'$ to $3'$ (260 to 390 pc) south of the optical center. However, the northern-most and southern-most extensions of the HI cloud do lie perfectly symmetrically above and below the declination of the center of the optical galaxy. Note that the small apparent optical diameter of Phoenix is a bit deceptive. The stellar distribution has been traced out to a radius of $8.7'$ (van de Rydt et al. 1991), so that the HI observed here is within the projected area of the Phoenix galaxy.

Figure 2 shows individual channel maps at $71''$ resolution; the curved shape of the HI in many of the channels and a gradual north-south velocity gradient are clearly evident. The peak brightness temperature (1.5 K) is not in the center of the cloud but in its southwest quadrant near $01^h 50^m 44^s$, $-44^{\circ} 29' 30''$. The peak column density ($5.4 \times 10^{19} \text{ cm}^{-2}$, or $0.6 M_{\odot} \text{ pc}^{-2}$ including He) is also here, so that the steepest radial gradients in column density are on the side opposite the stellar body. The peak brightness temperature at $71''$ resolution is only modestly higher than the brightness temperature at $133'' \times 102''$ resolution (1.4 K) even though the beam area is smaller by a factor of nearly 3, which suggests that the primary structures in the HI cloud are now resolved.

Figure 3 shows the velocity field of the HI emission; it also confirms general features noted in the channel maps and in the velocity field of St-Germain et al. (1999). The HI cloud shows a velocity gradient primarily in the north-south direction from -18 km s^{-1} on the north side towards -28 km s^{-1} in the south. Beyond -23 km s^{-1} the isovelocity contours bend towards the southeast, so that the most negative velocities are actually in the southeast corner of the cloud (east of $01^h 51^m$ and south of $-44^{\circ} 29'$). The integrated intensity image (Figure 1) also shows a protuberance on the west side of the HI cloud ($01^h 50^m 30^s$, $-44^{\circ} 29.5'$) which departs from the velocity trend noted above. Figure 3 shows that the protuberance has velocities of -20 km s^{-1} and higher; it is also visible in channel images at -12 , -15 , and -20 km s^{-1} . Even though this feature has quite low column density, only $1 \times 10^{19} \text{ cm}^{-2}$ at $71''$ resolution, it is clearly detected in both the ATCA observations of St-Germain et al. (1999) and in our VLA data, so it is undoubtedly real.

Fits of a Gaussian line profile to the data in velocities -2.0 km s^{-1} to -38.1 km s^{-1} give the velocity dispersions shown in Figure 4. Those HI dispersions range from 8 km s^{-1} to 14 km s^{-1} , and, to first order, most of the HI is consistent with a value of 10 km s^{-1} . There is a trend for larger dispersions to be found in the northern part of the cloud, and, aside from noisy regions at the edge of the galaxy, the dispersions are somewhat larger on the east side ($\sim 11 \text{ km s}^{-1}$) than on the west ($\sim 9 \text{ km s}^{-1}$). This trend, with larger dispersions on the side closer to the optical galaxy, is consistent with the pattern

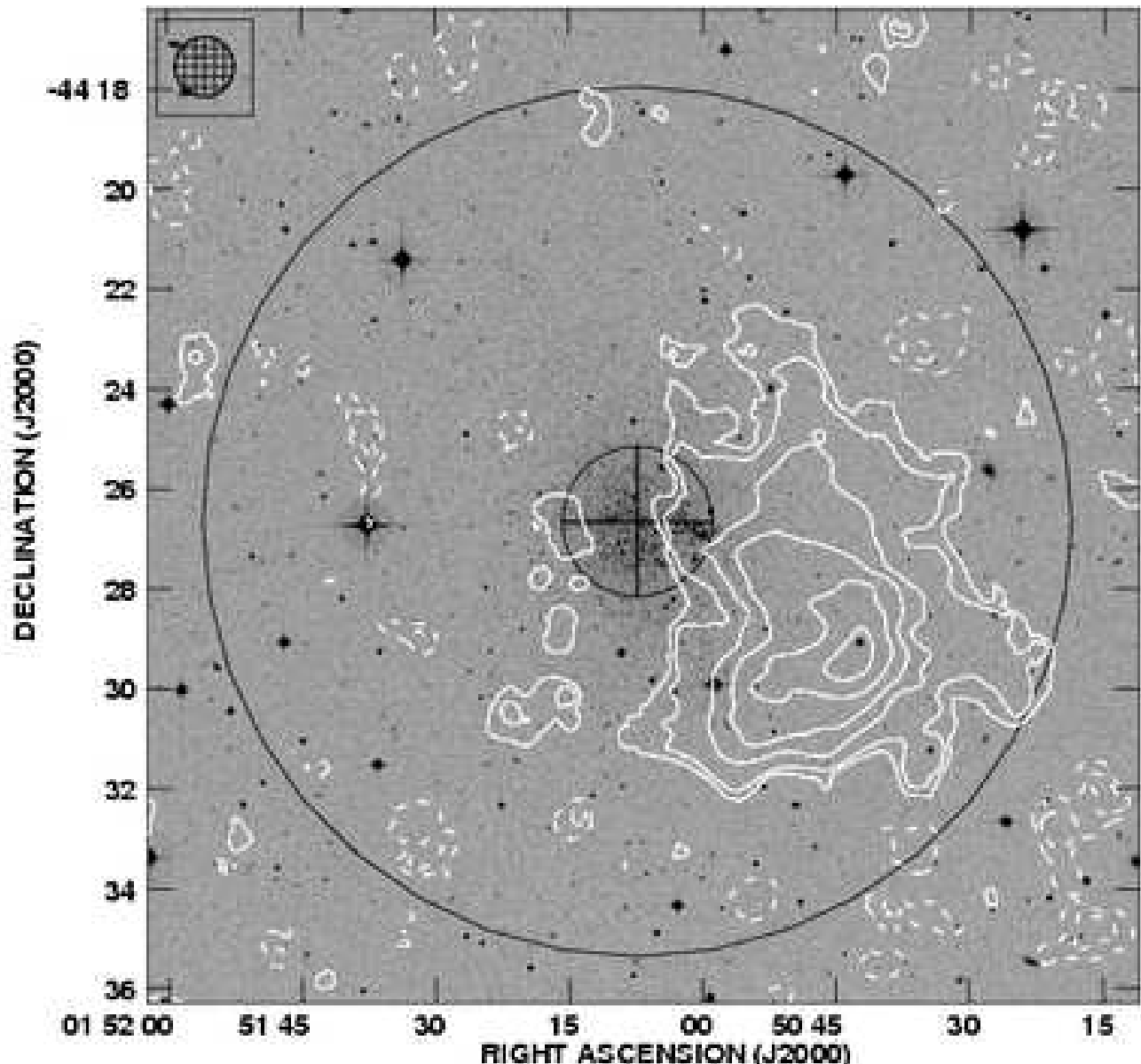


FIG. 1.— Integrated HI intensity at $71''$ resolution overlaid on the optical image of Phoenix from the DSS. Contours are $(-2, -1, -0.5, 0.5, 1, 2, 3, 4, \text{ and } 5) \times 10^{19} \text{ cm}^{-2}$. The small hashed circle in the top left corner indicates the resolution of the HI image. The crossed circle marks the bright part of the stellar distribution and is intended to guide the eye for a comparison with Figure 2. Note that the stellar distribution of Phoenix has been traced out to a radius of $8.7'$ (van de Rydt et al. 1991), as shown by the large circle, so that the HI observed here is within the projected area of the Phoenix galaxy.

expected from an expanding shell. Looking through the outside edge of the shell, the expansion velocity would be tangential to the line of sight and would not contribute to the line width; closer to the center of the expanding shell (on the north and east sides of the HI cloud, in this case) the expansion velocity would have some observable component and would broaden the line. However, if the HI cloud is an expanding shell its expansion velocity is only a few km s^{-1} and it is not possible to distinguish the expansion signature in position-velocity slices dominated by the overall N-S velocity gradient.

Neither our present data nor the results of St-Germain et al. (1999) give any hints for the presence of additional HI emission offset in any other direction from the optical galaxy, down to column density limits of approximately 10^{18} cm^{-2} at $130''$ resolution (40 times

smaller than the observed column densities). The significance of this non-detection lies mainly in the question of the importance of ram pressure as a gas removal mechanism. HI gas offset in multiple directions would almost certainly rule out ram pressure stripping as a credible explanation; however, we find no such gas.

In considering the possible effects of ram pressure on the gas in Phoenix, though, the morphology of the HI cloud is particularly interesting when compared to the morphology of HI in the dwarf galaxy Holmberg II (Bureau & Carignan 2002). The low resolution map of Ho II clearly shows smooth, convex, and compressed HI contours on the southeast side of the galaxy, with more irregular and fluffy low column density material extending to larger radii on the north and west sides. The cometary appearance of the HI in Ho II is clear evidence for the

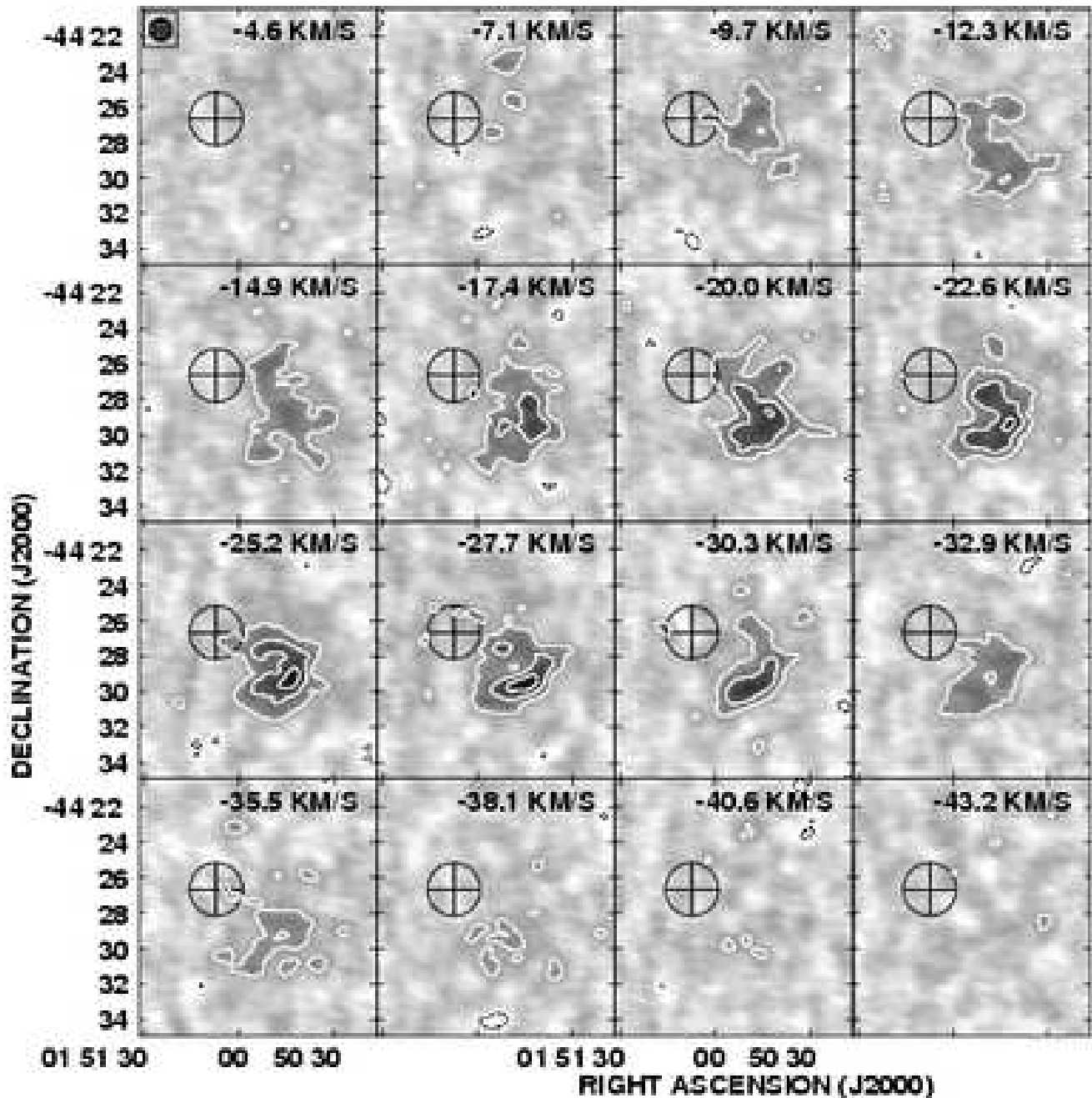


FIG. 2.— Channel maps at $71''$ resolution. Contours are -3 , 3 , 6 , and 9 times the rms noise (1.2 mJy b^{-1}). The resolution is indicated in the top left corner of the first panel, and the crossed circle shows the position and approximate size of the stellar body visible in the DSS image of Figure 1.

effects of ram pressure as the galaxy moves through the M81 intra-group medium. If ram pressure were responsible for displacing the HI from the center of Phoenix, we would expect to find a steeper HI column density gradient on the side towards the stellar body. We might also expect the cloud to have a convex side towards the stellar body. Neither of those is true, and thus the comparison with Ho II suggests that ram pressure is *not* responsible for the displacement of the HI in Phoenix.

Quantitatively, it is also unlikely that the density of the halo gas is high enough to effect any ram pressure stripping at Phoenix. In the usual manner we can

estimate the necessary density from the relation (e.g. Gunn & Gott 1972) $P_{\text{ram}} \sim \rho_{\text{halo}} v_{\text{gal}}^2 \sim GM_{\text{gal}} \Sigma_{\text{gas}} / R^2$, where v_{gal} is the velocity of the galaxy through the halo gas, M_{gal} is the mass of the galaxy interior to some radius R , and Σ_{gas} is the column density of the atomic gas there. Making the most conservative estimates for the HI properties of Phoenix we consider the outer edge of the HI cloud, which has surface density $0.1 M_{\odot} \text{ pc}^{-2}$ (including helium) at 590 pc from the galaxy center. We take Phoenix's mass to be $3.3 \times 10^7 M_{\odot}$ (Mateo 1998) and its velocity about the Milky Way approximately 220

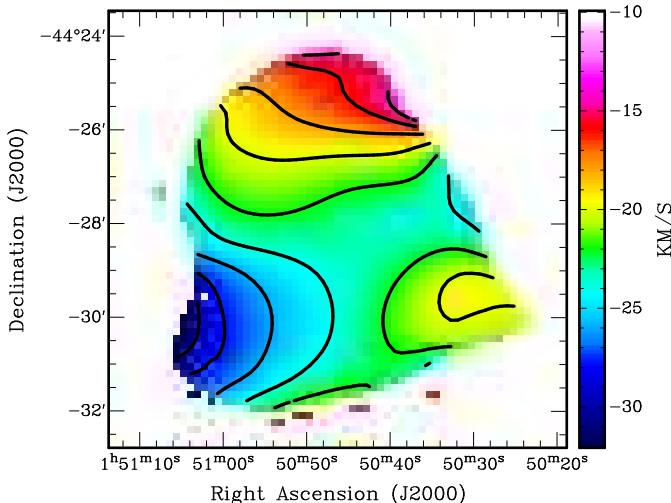


FIG. 3.— Velocity field, derived from fitting Gaussian line profiles to the image at $130''$ resolution. Contours range from -30 to -14 km s^{-1} in steps of 2 km s^{-1} .

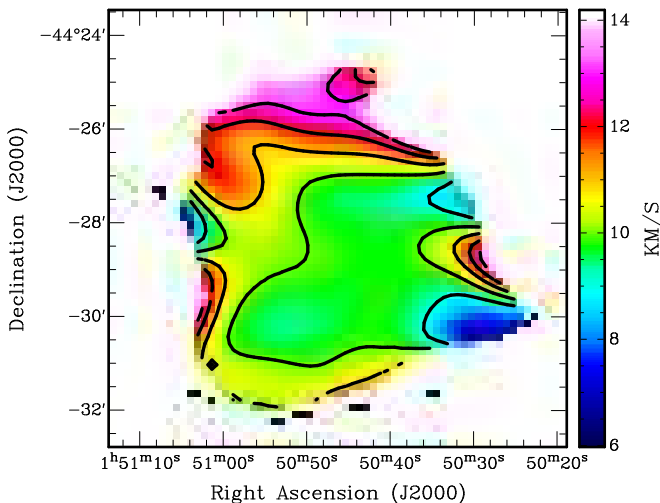


FIG. 4.— Velocity dispersion at $130''$ resolution. Contours range from 9 km s^{-1} to 13 km s^{-1} in steps of 1 km s^{-1} . Most of the HI can be characterized as having a velocity dispersion between ~ 9 and 11 km s^{-1} . A few pixels in which the formal uncertainty in the dispersion is greater than 2.5 km s^{-1} are not shown.

km s^{-1} . Stripping then requires the density of the halo gas to be $\rho_{\text{halo}} \gtrsim 3 \times 10^{-5} \text{ cm}^{-3}$. Stripping the gas of the highest observed column densities from the center of Phoenix requires at least an order of magnitude larger ρ_{halo} . Murali (2000) has estimated that the density of the Milky Way halo must be $\lesssim 10^{-5} \text{ cm}^{-3}$ at the location of the Magellanic Stream, however, and Phoenix is some eight times further from the Milky Way than that. Of course ram pressure stripping is easier if the mass of Phoenix has been overestimated, but by analogy with Marcolini et al. (2006), if the mass of Phoenix is very much smaller than we have assumed here it could not have retained its ISM long enough to support an extended star formation history.

Tidal stirring is another process which can be responsible for the removal of gas from a galaxy. However, since this process is most relevant at distances less than 50 kpc from the Milky Way (Mayer et al. 2006), the relative isolation of Phoenix makes this scenario unlikely. The radial velocity of -23 km s^{-1} corresponds to a galactocentric radial velocity of -112 km s^{-1} using the formulae presented in deVaucouleurs et al. (1991). At 112 km s^{-1} it has been at least 3 Gyr since Phoenix was close enough to the Milky Way for significant tidal interaction. If Phoenix is bound to the Milky Way, the semi-major axis of its orbit must be at least 210 kpc , giving an orbital period of 7.6 Gyr for a Milky Way mass of $1.4 \times 10^{12} M_{\odot}$ (Mateo 1998). Clearly, interactions with the Milky Way may have influenced Phoenix several Gyr ago but not more recently than that.

4. THE RECENT STAR FORMATION HISTORY OF THE PHOENIX DWARF

In an early ground-based optical study of Phoenix, Ortolani & Gratton (1988) noted the presence of a small ($\sim 10^4 M_{\odot}$) population of young ($\sim 10^8 \text{ yr}$) blue stars.² From deeper photometry, Martínez-Delgado, Gallart, & Aparicio (1999) (MGA) studied the distribution of these blue stars and found evidence of an east-to-west progression across the face of Phoenix. MGA estimated the age of these stars to be 100 Myr , and, from this, the relative position of the HI cloud detected by Young & Lo (1997), and the assumption that the HI cloud was associated with the recent star formation, estimated an outward velocity for the HI cloud of $\sim 7 \text{ km s}^{-1}$. At the time, the optical radial velocity of Phoenix was not known.

Gallart et al. (2001) obtained velocities for 31 Phoenix red giants and determined an optical radial velocity of -52 km s^{-1} . The $\sim 30 \text{ km s}^{-1}$ difference between the optical radial velocity and the HI radial velocity required a re-calculation of the estimated HI cloud velocity. The radial velocity difference implied a trajectory nearly along the line of sight, because placing the HI cloud back on top of the stars 100 Myr ago means the tangential velocity of the cloud is much less than 30 km s^{-1} . The resulting galaxy-HI cloud separation is 3.5 kpc . At this velocity and separation, the HI cloud is not bound to Phoenix (the mass estimate falls short by roughly one order of magnitude).

However, Irwin & Tolstoy (2002) obtained a new radial

² The abstract of the paper states 10^7 yr , but the text assigns an age of 10^8 yr .

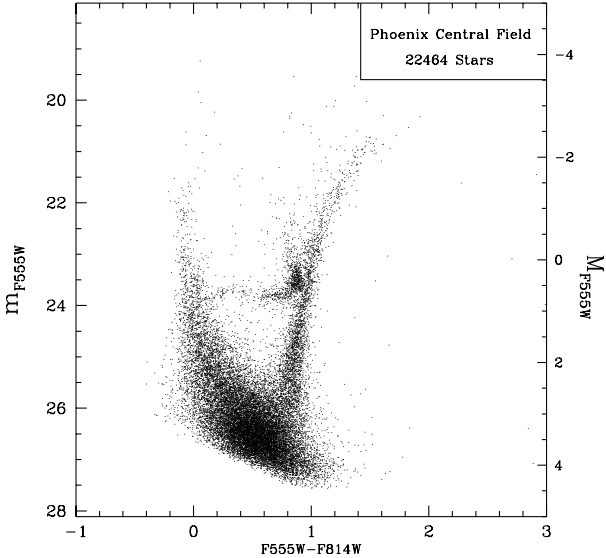


FIG. 5.— The V versus V-I color magnitude diagram from the HST WFPC2 observations of the central field of Phoenix (see text). The photometry comes from the Local Group Stellar Populations Archive (Holtzman et al. 2006). The right axis shows the absolute magnitude scale corresponding to the derived distance modulus of 23.11 ± 0.05 . Note the truncation in the main sequence at an apparent magnitude of ~ 21.5 . This provides an accurate determination of the age of the last star formation in Phoenix.

velocity of $-13 \pm 9 \text{ km s}^{-1}$, which is in excellent agreement with the HI velocity of -23 km s^{-1} . Held (2002) also reported agreement between the optical and HI radial velocities within $2 - 3 \text{ km s}^{-1}$. Thus, the original calculation by MGA would appear to be more relevant than that of Gallart et al. (2001) concerning the gravitational status of the HI cloud.

We have revisited the recent star formation history of the Phoenix dwarf in the following way. The Hubble Space Telescope WFPC2 has obtained relatively deep optical imaging of Phoenix in two different programs. Holtzman et al. (2000) report observations of a central field in Phoenix. They derive a star formation history for this field, and note that star formation proceeded in Phoenix up until 100 Myr ago, in agreement with Ortolani & Gratton (1988) and Martínez-Delgado, Gallart, & Aparicio (1999). Deeper HST WFPC2 observations of a central field which is almost coincident with that of Holtzman et al. were obtained by Aparicio (HST-GO-8706) in 2001. We have retrieved the photometry from these two Hubble Space Telescope observations of Phoenix from the HST/WFPC2 Local Group Stellar Photometry Archive (Holtzman et al. 2006). For reference, the V,V-I color magnitude diagram for the deeper integration is shown in Figure 5.

Using the programs of Dolphin (2002), we have derived the star formation histories for both Phoenix central field HST observations. In Figure 6 we show the total star formation history for the central field derived from the deeper integration. This star formation history agrees well with that derived from the slightly shallower integration and the analysis of those observations presented by Holtzman et al. (2000). There is evidence for a large

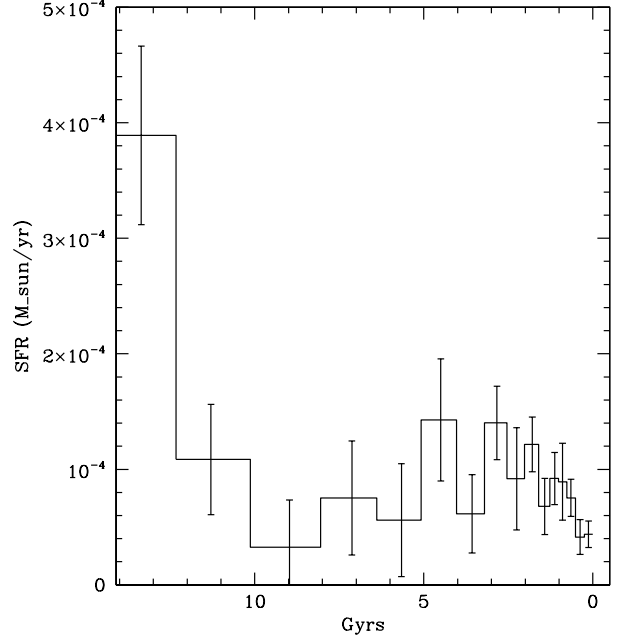


FIG. 6.— The global star formation history of the Phoenix dwarf galaxy derived from HST observations of a central field (see text). This star formation history is in generally good agreement with the central field star formation history derived by Holtzman et al. (2000).

amount of star formation at the earliest ages, a relative decrease at intermediate ages ($\sim 10 - 5 \text{ Gyr}$ ago), and then increased star formation activity in the last 5 Gyrs which decreases as the present time is approached.

In Figure 7 we show the star formation history for the last Gyr derived from the deeper integration at the higher time resolution afforded by the observations. The age of the last star formation event appears to be about 50 Myr ago with a duration of roughly 20 Myr. A similar analysis of the shallower central field observation gives a similar result. The age of 50 Myr for the most recent episode of star formation is slightly younger than the previous reported values of $\sim 100 \text{ Myr}$ ago. However, this is the first detailed analysis of this event from HST photometry, and Figure 5 shows that there is a clear truncation in the main sequence stars at an apparent V magnitude of ~ 21.5 , so the age estimate should be secure. Thus, it is likely that 50 Myr is a better estimate than 100 Myr for the most recent star formation event. Note that this most recent star formation episode is comparable in strength to the earlier episode at $\sim 200 \text{ Myr}$ ago. (Because linear time is plotted on the horizontal axis of Figure 7, the total star formation for any time is simply the area under the curve for the appropriate time bin.) Also note that the “gaps” in star formation at $\sim 300 \text{ Myr}$ and $\sim 100 \text{ Myr}$ ago are of similar duration ($\sim 50 \text{ Myr}$).

Using the age of 50 Myr for the most recent star formation event, we can calculate simple estimates of the HI cloud velocity and determine its gravitational status. The angular separation between the peak column density of the HI cloud and the optical center of the galaxy is $289''$. At a distance of 420 kpc, this corresponds to a projected distance of 590 pc. Under the assumptions that the HI cloud is 590 pc from the galaxy and was

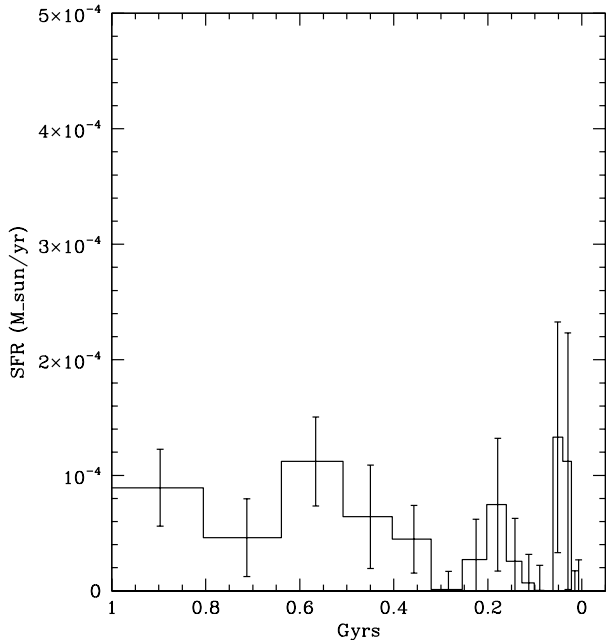


FIG. 7.— The recent star formation history of the Phoenix dwarf galaxy derived from HST observations of a central field (see text). The most recent episode of star formation has an age of roughly 50 Myr with no evidence of star formation since then.

expelled by the most recent episode of enhanced star formation, we derive a velocity of $\sim 12 \text{ km s}^{-1}$. An upper bound on the velocity and separation of the HI cloud can be obtained by including the observed radial velocity difference between HI and the stellar body (10 km s^{-1}); the recession speed of the HI cloud could be as large as 16 km s^{-1} and its true separation as large as 780 pc.

Given Phoenix’s total mass of $3.3 \times 10^7 M_{\odot}$ (Mateo 1998), the escape velocity for the HI cloud at the distance of 590 pc is 21 km s^{-1} . At 780 pc from Phoenix, the escape velocity is 19 km s^{-1} . The HI cloud’s velocity is $3\text{--}9 \text{ km s}^{-1}$ lower than the escape velocity, so we find that the cloud is still gravitationally bound. It is likely that the HI will fall back and may serve as the raw material for future episodes of star formation. However, we also note that there is an observed velocity difference of 12 km s^{-1} from one side of the cloud to the other, meaning that some portion of the cloud may be unbound. These conclusions are contradictory to those of Gallart et al. (2001), but this is purely a result of the previous authors’ use of a relatively large radial velocity offset between the HI and the stars.

For the observed HI mass, multiplied up by a factor of 1.3 to account for helium, and the recession velocities discussed above, we find that the total mechanical energy in the HI cloud is $2.3 \times 10^{50} - 3.9 \times 10^{50}$ ergs. Integrating over the star formation history, we calculate a total mass of $\sim 5 \times 10^3 M_{\odot}$ of new stars formed in the recent star formation event. For a standard IMF, one expects more than 10 stars with masses greater than $10 M_{\odot}$ formed in that event, so, even at low efficiency, there is sufficient energy available from the supernovae associated with the recent star formation to propel the HI away from the center of the galaxy.

Finally, there remains the question of why neutral gas

was only ejected to one side of Phoenix. Naively, one expects gas blown away by a burst of star formation to be ejected in all directions unless the energy source was initially off-center with respect to the gas. Could one off-center supernova be responsible for the asymmetric gas displacement in Phoenix? Assuming a canonical total energy for a supernova of 10^{51} erg implies an energy transfer efficiency in the range of 20%–40%. Note, however, that this efficiency does not take geometric effects into account — if the blast energy were injected symmetrically, much less than half of the 10^{51} erg would be available to accelerate a cloud off to one side of the supernova. Thus, our estimates are inconsistent with energy input from a single typical supernova. The idea also neglects the effects of the other ~ 10 supernovae that likely occurred. However, the combined effects of those supernovae could be responsible for the single-sided expulsion. Based on a comparison between the distributions of the brightest main sequence stars and the red supergiants, Martínez-Delgado, Gallart, & Aparicio (1999) found evidence for star formation propagating across Phoenix from east to west. The star formation wave may act as a plow to sweep up the gas and push it to one side of the galaxy.

We have investigated the HST observations to see if the detailed star formation history supports this interpretation of single-sided expulsion. The accuracy of the photometry of the main sequence stars in the HST photometry is substantially better than that of the ground based observation used by Martínez-Delgado, Gallart, & Aparicio (1999), so it is possible for us to examine the spatial distribution of main sequence stars as a function of luminosity (or upper age limit). In agreement with Martínez-Delgado, Gallart, & Aparicio (1999), we find the majority of the brightest main sequence stars fall in a band stretching across the middle of Phoenix. The brightest of these (stars with indicative ages of 25 - 75 Myr) are clustered in the association on the west side of the galaxy. Stars with older ages are more centrally concentrated. We also derived separate star formation histories for the eastern side of the galaxy and the western side of the galaxy. The western side shows evidence for strong episodes of star formation at 40 and 180 Myr ago preceded by star formation ~ 400 Myr ago. The eastern side shows evidence of relatively constant star formation at lower levels from 50 to 250 Myr ago and also star formation at ~ 450 Myr ago. In sum, the data are consistent with a general trend for the star formation propagating from east to west over the last 200 Myr, but the pattern is not a clear-cut, monotonic one (i.e., both sides of the galaxy participated in the star formation episode 200 Myr ago). These data are not inconsistent with the HI location on the west side of the galaxy.

5. DISCUSSION

The fact that the HI cloud appears to be bound to Phoenix is intriguing. From the asymmetrical shape of the HI cloud and the relative isolation of Phoenix, it appears that ram pressure stripping is not a likely cause of its displacement. Thus, supernova winds appear the most likely explanation for the HI cloud to be driven away from the center of the galaxy. However, if the HI cloud is bound, then $\sim 10^5 M_{\odot}$ of HI can fall back into

the galaxy, perhaps triggering a future episode of star formation.

Indeed, stellar population work has already suggested that this kind of a scenario (temporary HI expulsion, fall-back, and rejuvenated star formation) may have happened in the Carina dSph. Early on, Mould et al. (1982) noted that the presence of blue stars in the Carina dwarf indicated that Carina and possibly other dSphs were not single age systems. Further evidence for a complicated star formation history for Carina gathered (Saha et al. 1986; Mighell 1990; Smecker-Hane et al. 1994; Mighell 1997) until the present day picture of Carina consists of three episodes of star formation at roughly old, intermediate (7 Gyr) and young (3 Gyr) epochs (Hurley-Keller et al. 1998; Rizzi et al. 2003; Monelli et al. 2003). Two major questions which have always plagued studies of the star formation history of the Carina dSph are: (1) what caused the large gaps between the episodes of star formation, and (2) what removed the neutral gas from Carina such that there is no longer any star formation at all?

On the second question, the final clearing of gas from Carina and indeed the other dwarf spheroidals, Phoenix does not provide a direct answer because its HI is apparently still bound. The hydrodynamical simulations of Marcolini et al. (2006) and others also show that it is difficult for star formation activity, by itself, to blow out all of the ISM unless the dark matter halos are significantly smaller than expected and/or the hot gas's radiative energy losses much smaller. The simulations do tend to lift a significant component of the galaxy's cold gas up away from the stellar body in the aftermath (30 Myr – 50 Myr) of a burst, as we observe in Phoenix. But if star formation cannot completely unbind the ISM from a dwarf spheroidal, it is commonly assumed that some external agent such as tidal forces or ram pressure stripping must unbind the gas. This idea is certainly consistent with the fact that the most gas-poor dwarf spheroidals such as Draco and Ursa Minor tend to be closer to the Milky Way or to M31 than Phoenix is. A recent proper motion estimate for the Ursa Minor dwarf spheroidal implies that its perigalacticon is $\lesssim 50$ kpc (Piatek et al. 2005), carrying it well into the region where interactions with the Milky Way can clean it of its gas (Mayer et al. 2006). Piatek et al. (2005) have made the interesting comment, however, that perigalacticon distance cannot be the only factor influencing the evolution of a galaxy as the Carina and Ursa Minor dwarfs have similar orbits but quite different star formation histories.

With regard to the first question posed above, the origin of the gaps in the star formation activity of Carina, the Phoenix dwarf may be providing us with some answers. Here we posit that a relatively modest amount of star formation has lifted the neutral gas up out of the center of the potential well. However, most of the gas is not moving in excess of the escape velocity and is destined to return to the center. Again, from the separations and velocities discussed in §4 we can calculate the total energy (gravitational plus mechanical) of the HI cloud, the semi-major axis of its orbit and its orbital period. The estimated orbital periods are in the range 140 Myr to 660

Myr, so it seems reasonable that this mechanism could produce gaps in the star formation history on timescales of a few hundred Myr (Figure 7). On the 660 Myr orbit the semi-major axis is 1.2 kpc; thus, the HI cloud could reach angular separations several times larger than the current value.

Given the present distribution of the HI gas, it seems unlikely that it will all fall back in at once, so there may be some additional time delay as the gas collects before initiating the next episode of star formation. Since only $\sim 10^3 M_\odot$ of stars were formed in the episode that dislocated the gas, we may expect a similar amount of star formation when the $\sim 10^5 M_\odot$ of HI gas returns to the galaxy's center. Thus, the Phoenix dwarf may be aptly named.

6. SUMMARY

We have presented new VLA HI observations of the Local Group galaxy Phoenix. The galaxy has the properties of a dwarf spheroidal galaxy, with the exception that an HI cloud is located at a similar velocity and within the optical radius of the stellar distribution. The close association of the HI cloud with the galaxy suggests that this cloud may be the remnants of gas responsible for the most recent star formation in Phoenix which took place ≤ 100 Myr ago.

Our new high sensitivity and high resolution VLA HI imaging reveals that the HI distribution has a crescent-like shape with the center of curvature in the general direction of the galaxy. This indicates that ram pressure stripping is unlikely to be responsible for the displacement of the gas from the galaxy. Additionally, the isolation of the galaxy makes tidal stripping highly unlikely.

This leaves expulsion from the galaxy center by winds from supernovae as the most likely explanation. Using a star formation history constructed from HST imaging, we construct a simple kinematic model which implies that the HI cloud is still gravitationally bound to the galaxy. Much of the atomic gas can be expected to collect again in the center of the galaxy on timescales of a few hundred Myr. Thus, there may be future star formation in this dSph-like galaxy.

Support for this work was provided by NASA through grant AR-9251 from the Space Telescope Science Institute, which is operated by AURA, Inc., under NASA contract NAS5-26555. LY thanks New Mexico Tech for a sabbatical leave and appreciates the hospitality of the University of Oxford sub-department of Astrophysics, where part of this work was done. EDS is grateful for partial support from NASA LTSARP grant No. NAG5-9221 and from the University of Minnesota. DRW is grateful for support from a Penrose Fellowship. We also thank the referee for helpful comments. This research has made use of NASA's Astrophysics Data System Bibliographic Services and the NASA/IPAC Extragalactic Database (NED), which is operated by the Jet Propulsion Laboratory, California Institute of Technology, under contract with the National Aeronautics and Space Administration.

REFERENCES

- Briggs, D. S., Schwab, F. R., & Sramek, R. A. 1999, in *Synthesis Imaging in Radio Astronomy II*, eds. G. B. Taylor, C. L. Carilli, and R. A. Perley (ASP Conf. Ser., Vol. 180), pp 127–150
- Bureau, M., & Carignan, C. 2002, *AJ* 123, 1363

- de Boer, K. S., Braun, J. M., Vallenari, A., & Mebold, U. 1998, *A&A*, 329, L49
- Dekel, A., & Silk, J. 1986, *ApJ*, 303, 39
- deVaucouleurs, G., deVaucouleurs, A., Corwin, H. G., Jr., Buta, R. J., Paturel, G., & Fouque, P. 1991, *Third Reference Catalog of Bright Galaxies*, Springer-Verlag.
- Dolphin, A. E. 2002, *MNRAS*, 332, 91
- Dolphin, A. E., Weisz, D. R., Skillman, E. D., & Holtzman, J. A., in *Resolved Stellar Populations*, eds. D. Valls-Gabaud & M. Chavez, *ASP Conf. Ser.*, in press (astro-ph/0506430)
- Einasto, J., Kaasik, A., & Saar, E. 1974, *Nature*, 250, 309
- Fenner, Y., Gibson, B. K., Gallino, R., & Lugaro, M. 2006, *ApJ*, 646, 184
- Gallart, C., Martínez-Delgado, D., Gómez-Flechoso, M. A., & Mateo, M. 2001, *AJ*, 121, 2572
- Grebel, E. K. 2001, *Astrophysics and Space Science Supplement*, 277, 231
- Gunn, J. E., & Gott, J. R. III, 1972, *ApJ*, 176, 1
- Held, E. V. 2002, *Scientific Drivers for ESO Future VLT/VLTI Instrumentation: Proceedings of the ESO Workshop Held in Garching, Germany, 11-15 Juni 2001*, ESO ASTROPHYSICS SYMPOSIA. ISBN 3-540-43755-X. Edited by J. Bergeron and G. Monnet. Springer-Verlag, 2002, p. 178, 178
- Held, E. V., Saviane, I., & Momany, Y. 1999, *A&A*, 345, 747
- Holtzman, J. A., Smith, G. H., & Grillmair, C. 2000, *AJ*, 120, 3060
- Holtzman, J. A., Afonso, C., & Dolphin, A., *ApJ*, in press
- Hurley-Keller, D., Mateo, M., & Nemeč, J. 1998, *AJ*, 115, 1840
- Ikuta, C., & Arimoto, N. 2002, *A&A*, 391, 55
- Irwin, M., & Tolstoy, E. 2002, *MNRAS*, 336, 643
- Klypin, A., Kravtsov, A. V., Valenzuela, O., & Prada, F. 1999, *ApJ*, 522, 82
- Kormendy, J. 1985, *ApJ*, 295, 73
- Larson, R. B. 1974, *MNRAS*, 169, 229
- Lin, D. N. C., & Faber, S. M. 1983, *ApJ*, 266, L21
- Mac Low, M.-M., & Ferrara, A. 1999, *ApJ*, 513, 142
- Marcolini, A., D'Ercole, A., Brighenti, F., & Recchi, S. 2006, *MNRAS*, 371, 643
- Martínez-Delgado, D., Gallart, C., & Aparicio, A. 1999, *AJ*, 118, 862
- Mateo, M. L. 1998, *ARA&A*, 36, 435
- Mayer, L., Governato, F., Colpi, M., Moore, B., Quinn, T., Wadsley, J., Stadel, J., & Lake, G. 2001a, *ApJ*, 547, L123
- Mayer, L., Governato, F., Colpi, M., Moore, B., Quinn, T., Wadsley, J., Stadel, J., & Lake, G. 2001b, *ApJ*, 559, 754
- Mayer, L., Mastropietro, C., Wadsley, J., Stadel, J., & Moore, B. 2006, *MNRAS*, 369, 1021
- Mighell, K. J. 1990, *A&AS*, 82, 1
- Mighell, K. J. 1997, *AJ*, 114, 1458
- Monelli, M., et al. 2003, *AJ*, 126, 218
- Moore, B., Governato, F., Quinn, T., Stadel, J., & Lake, G. 1998, *ApJ*, 499, L5
- Mould, J. R., Cannon, R. D., Frogel, J. A., & Aaronson, M. 1982, *ApJ*, 254, 500
- Murali, C. 2000, *ApJ*, 529, 81
- Ortolani, S., & Gratton, R. G. 1988, *PASP*, 100, 1405
- Piatek, S., Pryor, C., Bristow, P., Olszewski, E. W., Harris, H. C., Mateo, M., Minniti, D., & Tinney, C. G. 2005, *AJ*, 130, 95
- Rizzi, L., Held, E. V., Bertelli, G., & Saviane, I. 2003, *ApJ*, 589, L85
- Saha, A., Monet, D. G., & Seitzer, P. 1986, *AJ*, 92, 302
- Smecker-Hane, T. A., Stetson, P. B., Hesser, J. E., & Lehnert, M. D. 1994, *AJ*, 108, 507
- St-Germain, J., Carignan, C., Côte, S., & Oosterloo, T. 1999, *AJ*, 118, 1235
- Vader, J. P. 1986, *ApJ*, 305, 669
- van den Bergh, S. 1994, *AJ*, 107, 1328
- van den Bergh, S. 1994, *ApJ*, 428, 617
- van de Rydt, F., Demers, S., & Kunkel, W. E. 1991, *AJ*, 102, 130
- Venn, K. A., Irwin, M., Shetrone, M. D., Tout, C. A., Hill, V., & Tolstoy, E. 2004, *AJ*, 128, 1177
- Young, L. M., & Lo, K. Y. 1997, *ApJ*, 490, 710